Sum Throughput Maximization for Heterogeneous Multicell Networks with RF-Powered Relays

Ali A. Nasir*, Duy T. Ngo†, Xiangyun Zhou*, Rodney A. Kennedy*, and Salman Durrani*

*Research School of Engineering, Australian National University, Canberra, Australia
Email: {ali.nasir, xiangyun.zhou, rodney.kennedy, salman.durrani}@anu.edu.au.
†School of Electrical Engineering & Computer Science, University of Newcastle, Australia. Email: duy.ngo@newcastle.edu.au.

Abstract—**This paper considers a heterogeneous multicell network where the base station (BS) in each cell communicates with its cell-edge user with the assistance of an amplify-and-forward relay node. Equipped with a power splitter and a wireless energy harvester, the relay scavenges RF energy from the received signals to process and forward the information. In the face of strong intercell interference and limited radio resources, we develop a resource allocation scheme that jointly optimizes (i) BS transmit powers, (ii) power splitting factors for energy harvesting and information processing at the relays, and (iii) relay transmit powers. To solve the highly non-convex problem formulation of sum-rate maximization, we propose to apply the successive convex approximation (SCA) approach and devise an iterative algorithm based on geometric programming. The proposed algorithm transforms the nonconvex problem into a sequence of convex problems, each of which is solved very efficiently by the interior-point method. We prove that our developed algorithm converges to an optimal solution that satisfies the Karush-Kuhn-Tucker conditions of the original nonconvex problem. Numerical results confirm that our joint optimization solution substantially improves the network performance, compared to the existing solution wherein only the received power splitting factors at the relays are optimized.**

I. INTRODUCTION

Heterogeneous multicell networks have been proposed as a promising solution for 5G communication standard [1]. In multicell networks, users at the cell edges can experience poor signal reception being out-of-direct-communication-range from the base stations (BSs) and due to strong intercell interference. The viable solution to this critical issue is the opportunistically deployed relays which connect to the macrocell BSs via wireless links and provide network coverage to the cell-edge users [2]. In addition, the performance of a heterogeneous multicell network is further enhanced with coordinated multipoint transmission and reception (CoMP) techniques, in which BSs and relays cooperate with one another to best serve the cell-edge users [3].

The opportunistic nature of relay deployments may restrict the access to a main power supply. This problem can be circumvented by implementing wireless energy harvesting techniques at the relays, where energy is scavenged from the ambient propagating electromagnetic waves in the radio frequency (RF) [4]–[8]. Wireless energy harvesting solutions are feasible for heterogeneous relays, which only require significantly low transmit power due to their restricted network coverage [9].

In a heterogeneous multicell network with RF-powered relays, the key factors that determine the system performance include:

(i) how effectively the intercell interference is managed, (ii) how the limited transmit power is allocated at the BSs, and (iii) how the harvested RF energy is utilized at the relays. Existing research efforts have partially addressed these central issues. Considering the downlink of a multicell multiuser interference network, [10] proposed coordinated scheduling and power control algorithms for the macrocell BSs only. In [11], resource allocation schemes were specifically developed for the remote radio heads—a form of heterogeneous relays. Assuming simultaneous wireless information and power transfer, [12] considered the power control problem for multiuser broadband wireless systems without relays. In [13], an optimal power splitting rule was devised for energy harvesting and information processing at the self-sustaining relays of a multiuser interference network. However, [13] did not address the important issue of optimally controlling the transmit powers at the BSs and the relays.

In this paper, we consider a heterogeneous multicell network in which the BS in each cell communicates with its cell-edge user via the assistance of an energy-constrained relay node. Employing CoMP, we assume that multiple BSs cooperate to share the channel quality measurements and to schedule the transmissions, allowing for more efficient radio resource utilization. Each relay in multicell network is equipped with a wireless energy harvester that scavenges part of the RF energy in the received signal. A power splitter is included in the relay to decide the portion of the received signal energy to be harvested. Using the harvested energy, an information transceiver will later amplify and forward (AF) the received signal to its corresponding user. Our aim is to devise an optimal resource allocation policy for both the BSs and the energy-harvesting relays in order to maximize the network sum throughput. Different from the existing works, we jointly optimize the transmit powers at the BSs and the relays, along with finding an optimal power splitting rule for energy harvesting and signal processing at the relays. Since the optimization variables are strongly coupled with many nonlinear cross-multiplying terms, the formulated problem is highly nonconvex and thus challenging to solve. The main contributions of this work are:

- We propose to adopt the successive convex approximation (SCA) method and transform the problem to a series of convex programs. Here, we specifically tailor the generic SCA framework to allow for the application of geometric programming (GP). To arrive at the convex program, we use the arithmetic-geometric inequality to condense a posynomial to a monomial. At each step of our proposed iterative

algorithm, we efficiently solve the resulting convex problem by the interior-point method.

- We prove that our developed algorithm generates a sequence of improved feasible solutions, which eventually converges to the solutions that satisfy the Karush-Kuhn-Tucker (KKT) conditions of the original nonconvex problem. While a true globally optimal method does not exist for the formulated problem, it is noted that SCA-based solution often empirically achieves the global optimum in most practical scenarios [14]–[16].
- We confirm via numerical examples that our joint optimization approach significantly outperforms the existing solution that only optimizes how the received power is split at the relays.

II. SYSTEM MODEL AND PROBLEM FORMULATION

Consider the downlink transmissions in an N-cell heterogeneous network with universal frequency reuse, i.e., the same radio frequencies are used in all cells. We adopt CoMP and assume that the base stations (BSs) are connected to a central processing (CP) unit which coordinates the multicellular transmissions and radio resource management. Let $\mathcal{N} = \{1, \ldots, N\}$ denote the set of all cells. In a cell $i \in \mathcal{N}$, the BS attempts to establish communication with its single cell-edge user. Assume that the N users in the network are located in the 'signal dead zones', where no direct signal from any BSs can reach. To provide the network coverage to these distant users, a relay node is deployed in each cell to assist the communication from the BS to its user. Denote the channel coefficient from BS i to relay j as $h_{i,j}$, and that from relay j to user k as $g_{j,k}$. We assume that all BSs send the available channel state information to the CP unit via a dedicated control channel. In Fig. 1, an example 3-cell heterogenous network with relays is illustrated.[1]

The relays are assumed to be energy-constrained nodes, i.e., they do not have any energy supply of their own. Each of these relays is equipped with a wireless energy harvester that scavenges energy in the received RF signals from all BSs (including its servicing BS and other interfering BSs). At each relay, the harvested energy is used by an information transceiver to process and forward the message signal to the intended user.

We propose to divide the total transmission block time T into two equal time slots. The first time slot includes BS-to-relay transmissions and RF energy harvesting at the relays. This is done while all the relays do not transmit. The second time slot includes signal processing at the relays and relay-to-user transmissions. This is done while all the BSs suppress their transmissions. The operations in each time slot are illustrated in Fig. 2, which will be detailed in the following subsections.

A. BS-to-Relay Transmissions and Wireless Energy Harvesting at Relays

In the first time slot $[0, T/2]$, let x_i be the normalized information signal sent by BS i, i.e., $\mathbb{E}\{|x_i|^2\} = 1$, where $\mathbb{E}\{\cdot\}$ denotes the expectation operator and $|\cdot|$ the absolute value operator. Let P_i be the transmit power of BS i, $d_{i,j}^h$ the

---

[1]Note that the network analysis and proposed solutions in this paper are general; hence, they are valid for any cellular network geometry and can be straightforwardly extended to the case of multiple relays and multiple users in a cell.
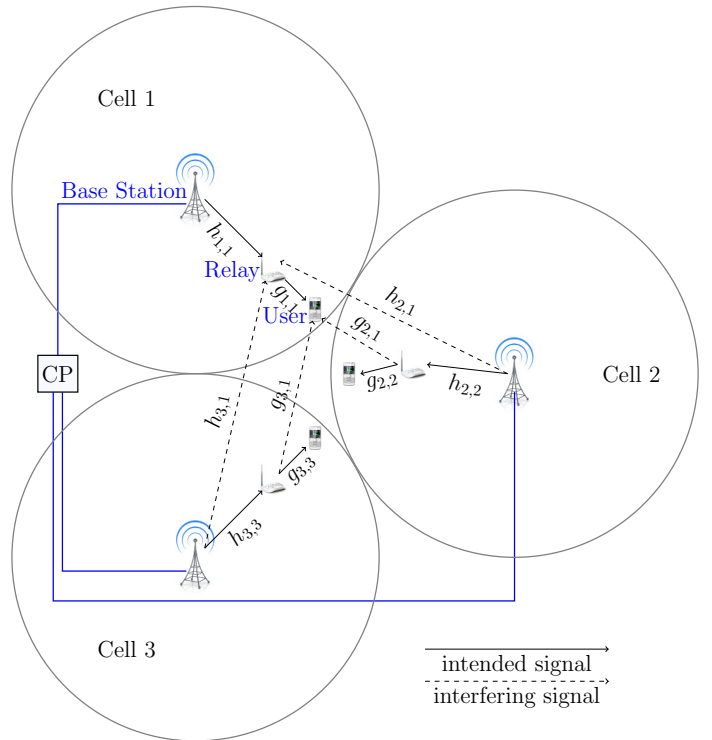

Fig. 1. An example heterogeneous multicell network consisting of three cells and a central processing (CP) unit. Each cell has a base station, a relay and a cell-edge user. For clarity, we only show the interfering scenarios in cell 1, i.e., at the receivers of relay 1 and user 1. In general, the interference occurs at the receivers of all three relays and three users.

distance between BS i and relay j, and β the path-loss exponent. Assuming that n_i^a is the zero-mean additive white Gaussian noise (AWGN) with variance σ_i^a at the receive antenna of relay i, the received signal at relay i can be expressed as

$$y_{R_i} = \bar{h}_{i,i}\sqrt{P_i}x_i + \sum_{j=1, j\neq i}^{N} \bar{h}_{j,i}\sqrt{P_j}x_j + n_i^a, \quad (1)$$

where $\bar{h}_{j,i} \triangleq h_{j,i}\left(d_{j,i}^h\right)^{-\beta/2}$, $\forall i, j \in \mathcal{N}$, is the effective channel gain from BS j to relay i (including the effects of both small-scale fading and large-scale path loss).

To implement dual energy harvesting and signal processing at the relays, we assume that each relay is equipped with a power splitter that determines how much received signal energy should be dedicated to each of the two purposes [5], [7], [13]. As shown in Fig. 2, the power splitter at relay $i \in \mathcal{N}$ divides the power of y_{R_i} into two parts in the proportion of $\alpha_i : (1 - \alpha_i)$. Here, $\alpha_i \in (0, 1)$ is termed as the power splitting factor. The first part $\sqrt{\alpha_i}y_{R_i}$ is processed by the energy harvester and stored as energy (e.g., by charging a battery at relay i) for the use in the second time slot. The amount of energy harvested at relay i is given by

$$E_i = \frac{\eta\alpha_i T}{2} \sum_{j=1}^{N} P_j|\bar{h}_{j,i}|^2, \quad (2)$$

where $\eta \in (0, 1)$ is the efficiency of energy conversion.

The second part $\sqrt{1 - \alpha_i}y_{R_i}$ of the received signal is passed to an information transceiver. In Fig. 2, n_i^r denotes the AWGN
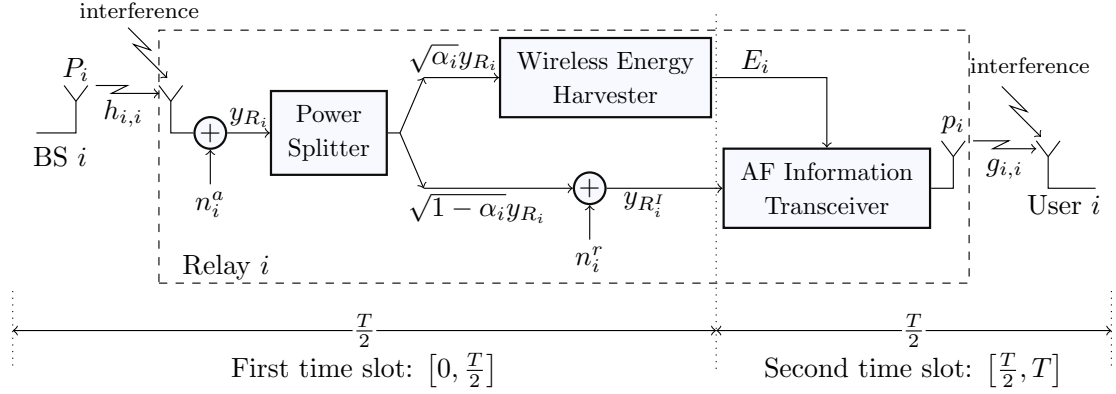
Fig. 2. BS-to-user communication assisted by a RF-powered relay

with zero mean and variance σ_i^r introduced by the baseband processing circuitry. Since antenna noise power σ_i^a is very small compared to the circuit noise power σ_i^r in practice [17], n_i^a has a negligible impact on both the energy harvester and the information transceiver of relay i. For simplicity, we will thus ignore the effect of n_i^a in the following analysis by setting $\sigma_i^a = 0$. The signal at the input of the information transceiver of relay i can be written as

$$y_{R_i}^I = \sqrt{1-\alpha_i}\,y_{R_i} + n_i^r$$
$$= \sqrt{1-\alpha_i}\bar{h}_{i,i}\sqrt{P_i}x_i + \sqrt{1-\alpha_i}\sum_{j=1,j\neq i}^N \bar{h}_{j,i}\sqrt{P_j}x_j + n_i^r, \quad (3)$$

where the first term in (3) is the desired signal from BS i, and the second term is the total interference from all other BSs.

B. Signal Processing at Relays and Relay-to-User Transmissions

In the second time slot $[T/2, T]$, the information transceiver amplifies the signal $y_{R_i}^I$ prior to forwarding it to user i. Denote the transmit power of relay transceiver i as p_i. With the harvested energy E_i in (2), the maximum power available for transmission at relay i is given by $\frac{E_i}{T/2}$, which means that

$$p_i \leq \frac{2E_i}{T} = \eta\alpha_i\sum_{j=1}^N P_j|\bar{h}_{j,i}|^2. \quad (4)$$

The transmitted signal from relay i to user i is given by

$$x_{R_i} = \zeta_i\sqrt{p_i}\,y_{R_i}^I, \quad (5)$$

where $\zeta_i \triangleq \left[(1-\alpha_i)\sum_{j=1}^N P_j\bar{h}_{j,i} + \sigma_i^r\right]^{-1/2}$ is the amplifying factor that ensures power constraint (4) be met.

The received signal at user i is then give by

$$y_{U_i} = \bar{g}_{i,i}x_{R_i} + \sum_{j=1,j\neq i}^N \bar{g}_{j,i}x_{R_j} + n_i^u, \quad (6)$$

where $\bar{g}_{j,i} \triangleq g_{j,i}\left(d_{j,i}^g\right)^{-\beta/2}$, $\forall i,j \in \mathcal{N}$, is the effective channel gain from BS j to relay i (including the effects of both small-scale fading and large-scale path loss), $d_{i,j}^g$ denotes the distance between relay i and user j, n_i^u the AWGN with zero mean and variance σ_i^u at the receiver of user i. Using x_{R_i} in (5) and $y_{R_i}^I$ in (3), we can write (6) explicitly as

$$y_{U_i} = \zeta_i\bar{g}_{i,i}\bar{h}_{i,i}\sqrt{p_iP_i(1-\alpha_i)}x_i$$
$$+ \zeta_i\bar{g}_{i,i}\sqrt{p_i(1-\alpha_i)}\sum_{j=1,j\neq i}^N \bar{h}_{j,i}\sqrt{P_j}x_j$$
$$+ \zeta_i\bar{g}_{i,i}\sqrt{p_i}n_i^r + \sum_{j=1,j\neq i}^N \zeta_j\bar{g}_{j,i}\sqrt{p_j}y_{R_j}^I + n_i^u. \quad (7)$$

The first term in (7) is the desired signal from BS i to its serviced user i, and the remaining terms represent the total intercell interference and noise.

Without loss of generality, let us assume $\sigma_i^r = \sigma_i^u = \sigma$, $\forall i \in \mathcal{N}$. From (7), the signal-to-interference-plus-noise ratio (SINR) at the receiver of user i is given in (8) [see the bottom of this page], where we define

$$\phi_1^{i,j} \triangleq \frac{|\bar{g}_{i,i}\bar{h}_{j,i}|^2}{\sigma^2}; \quad \phi_2^{i,j} \triangleq \frac{|\bar{h}_{j,i}|^2}{\sigma};$$
$$\phi_3^{i,j} \triangleq \frac{|\bar{g}_{j,i}|^2}{\sigma}; \quad \phi_4^{i,j,k} \triangleq \frac{|\bar{g}_{j,i}\bar{h}_{k,i}|^2}{\sigma^2}. \quad (9)$$

For notational convenience, let us also define $\mathbf{P} \triangleq [P_1,\ldots,P_N]^T$, $\mathbf{p} \triangleq [p_1,\ldots,p_N]^T$, and $\boldsymbol{\alpha} \triangleq [\alpha_1,\ldots,\alpha_N]^T$. From (8), the achieved throughput in bps/Hz (bits per second per Hz) of cell i is then:

$$\tau_i(\mathbf{P},\mathbf{p},\boldsymbol{\alpha}) = \frac{1}{2}\log_2(1+\gamma_i). \quad (10)$$

An important observation from (8) and (10) is that by dedicating more received power at relay i for energy harvesting (i.e. increasing α_i), one might actually degrade the end-to-end throughput in cell i. This can be verified upon dividing both

$$\gamma_i = \frac{\phi_1^{i,i}P_ip_i(1-\alpha_i)}{\displaystyle\sum_{j=1,j\neq i}^N \phi_1^{i,j}P_jp_i(1-\alpha_i) + \sum_{j=1}^N\left(\phi_2^{i,j}P_j(1-\alpha_i) + \phi_3^{i,j}p_j\right) + \sum_{j=1,j\neq i}^N\sum_{k=1}^N \phi_4^{i,j,k}P_kp_j(1-\alpha_i) + 1}, \quad (8)$$

the numerator and the denominator of γ_i in (8) by $(1 - \alpha_i)$. However if one opts to decrease α_i, the transmit power available at the information transceiver of relay i will be further limited [see (4)], thus potentially reducing the corresponding data rate τ_i. Similarly, increasing the BS transmit power P_i or the relay transmit power p_i does not necessarily enhance the throughput τ_i of cell i. The reason is that P_i and p_i appear in the positive terms at both the numerator and the denominator of γ_i. These observations emphasize the importance of finding an optimal resource allocation policy for the considered network.

In this paper, we will devise an optimal tradeoff of all three parameters—transmit power $\mathbf{P}$ at the BSs, transmit power $\mathbf{p}$ at the relays, and power splitting factor $\boldsymbol{\alpha}$ at the relays. With the objective of maximizing the total network throughput, the design problem is formulated as follows

$$\max_{\mathbf{P},\mathbf{p},\boldsymbol{\alpha}} \quad \sum_{i=1}^{N} \tau_i \tag{11a}$$

$$\text{s.t.} \quad 0 \leq \alpha_i \leq 1, \quad \forall i \in \mathcal{N} \tag{11b}$$

$$P_{\min} \leq P_i \leq P_{\max}, \quad \forall i \in \mathcal{N} \tag{11c}$$

$$0 \leq p_i \leq \eta \alpha_i \sum_{j=1}^{N} P_j |\bar{h}_{j,i}|^2, \quad \forall i \in \mathcal{N}, \tag{11d}$$

where $P_{\max}$ denotes the maximum power available for transmission at each BS and $P_{\min}$ is the minimum transmit power required at each BS to ensure the activation of energy harvesting circuitry at the relay. In this formulation, (11b) is the constraint for the power splitting factors at all relays. Constraints (11c) and (11d) ensure that the transmit powers at the BSs and relays do not exceed the maximum allowable.

Problem (11) is highly nonconvex in $(\mathbf{P}, \mathbf{p}, \boldsymbol{\alpha})$ because the throughput τ_i in (10) is highly nonconvex in these three variables. Even if we fix $\mathbf{p}$ and $\boldsymbol{\alpha}$ and try to optimize $\mathbf{P}$ alone, τ_i would still be highly nonconvex in $\mathbf{P}$ due to the cross-cell interference terms. Simultaneously optimizing $\mathbf{P}, \mathbf{p}$ and $\boldsymbol{\alpha}$ is much more challenging due to the nonlinearity introduced by the cross-multiplying terms, e.g., $P_k p_j \alpha_i$ in (8) and $\alpha_i P_j$ in (11d).

III. PROPOSED SCA SOLUTION USING GEOMETRIC PROGRAMMING

To efficiently solve (11), we propose to adopt the successive convex approximation (SCA) approach [14]–[16] to transform the original nonconvex problems into a sequence of convex subproblems. For our formulated problem, the key steps of the generic SCA framework are summarized in Algorithm 1 [18]. In applying the SCA approach, there still remain two key questions:

1) How do we perform the approximation in Steps 2 and 4 of Algorithm 1?
2) Given that the approximation is known, can we prove that the resulting algorithm converges to an optimal solution?

To answer the first question, we will make use of the single condensation approximation method [14] to form a relaxed geometric program (GP), instead of directly solving the nonconvex problems (11). A GP is expressed in the standard form as [19,

---

Algorithm 1 Successive Convex Approximation

1: Initialize with a feasible solution $(\mathbf{P}^{[0]}, \mathbf{p}^{[0]}, \boldsymbol{\alpha}^{[0]})$.
2: At the m-th iteration, form a convex subproblem by approximating the nonconcave objective function and constraints of (11) with some concave function around the previous point $(\mathbf{P}^{[m-1]}, \mathbf{p}^{[m-1]}, \boldsymbol{\alpha}^{[m-1]})$.
3: Solve the resulting convex subproblem to obtain an optimal solution $(\mathbf{P}^{[m]}, \mathbf{p}^{[m]}, \boldsymbol{\alpha}^{[m]})$ at the m-th iteration.
4: Update the approximation parameters in Step 2 for the next iteration.
5: Go back to Step 2 and repeat until $(\mathbf{P}, \mathbf{p}, \boldsymbol{\alpha})$ converges.

$$\min_{\mathbf{y}} \quad f_0(\mathbf{y}) \tag{12a}$$

$$\text{s.t.} \quad f_i(\mathbf{y}) \leq 1, \quad i = 1, \ldots, m \tag{12b}$$

$$h_\ell(\mathbf{y}) = 1, \quad \ell = 1, \ldots, M \tag{12c}$$

where $f_i(\mathbf{y})$, $i = 0, \ldots, m$ are posynomials and $h_\ell(\mathbf{y})$, $\ell = 1, \ldots, M$ are monomials[2]. A GP in standard form is a nonlinear and nonconvex optimization problem because posynomials are not convex functions. However, with a logarithmic change of the variables and multiplicative constants, one can turn it into an equivalent nonlinear and convex optimization problem (using the property that the log-sum-exp function is convex) [14], [19].

First, we express the objective function (11a) as

$$\max_{\mathbf{P},\mathbf{p},\boldsymbol{\alpha}} \sum_{i=1}^{N} \frac{1}{2} \log_2(1 + \gamma_i) \equiv \max_{\mathbf{P},\mathbf{p},\boldsymbol{\alpha}} \log_2 \prod_{i=1}^{N} (1 + \gamma_i) \tag{13a}$$

$$\equiv \min_{\mathbf{P},\mathbf{p},\boldsymbol{\alpha}} \prod_{i=1}^{N} \frac{1}{1 + \gamma_i}, \tag{13b}$$

where (13b) follows from (13a) because $\log(\cdot)$ is monotonically increasing function. Upon substituting γ_i in (8) to (13b) and replacing $1 - \alpha_i$ by an auxiliary variable t_i, it is shown that problem (11) is equivalent to (14) [see the top of the next page], where $\mathbf{t} \triangleq [t_1, \cdots, t_N]^T$.

It can be seen that (14) is not yet in the form of the GP (12) because (14a) and (14d) are not posynomials. Now, let us define:

$$u_i(\mathbf{x}) \triangleq \sum_{j=1,j\neq i}^{N} \phi_1^{i,j} P_j p_i t_i + \sum_{j=1}^{N} \left(\phi_2^{i,j} P_j t_i + \phi_3^{i,j} p_j \right)$$
$$+ \sum_{j=1,j\neq i}^{N} \sum_{k=1}^{N} \phi_4^{i,j,k} P_k p_j t_i + 1, \tag{15}$$

$$v_i(\mathbf{x}) \triangleq \sum_{j=1}^{N} \left(\phi_1^{i,j} P_j p_i t_i + \phi_2^{i,j} P_j t_i + \phi_3^{i,j} p_j \right)$$
$$+ \sum_{j=1,j\neq i}^{N} \sum_{k=1}^{N} \phi_4^{i,j,k} P_k p_j t_i + 1, \tag{16}$$

---

[2]A monomial $q(\mathbf{y})$ is defined as $q(\mathbf{y}) \triangleq c y_1^{a_1} y_2^{a_2} \ldots y_n^{a_n}$, where $c > 0$, $\mathbf{y} = [y_1, y_2, \ldots, y_n]^T \in \mathbb{R}_{++}^n$, and $\mathbf{a} = [a_1, a_2, \ldots, a_n]^T \in \mathbb{R}^n$. A posynomial is a nonnegative sum of monomials [19].

$$\min_{\mathbf{P},\mathbf{p},\boldsymbol{\alpha},\mathbf{t}} \quad \prod_{i=1}^{N} \frac{\sum_{j=1,j\neq i}^{N} \phi_1^{i,j} P_j p_i t_i + \sum_{j=1}^{N}\left(\phi_2^{i,j} P_j t_i + \phi_3^{i,j} p_j\right) + \sum_{j=1,j\neq i}^{N}\sum_{k=1}^{N} \phi_4^{i,j,k} P_k p_j t_i + 1}{\sum_{j=1}^{N}\left(\phi_1^{i,j} P_j p_i t_i + \phi_2^{i,j} P_j t_i + \phi_3^{i,j} p_j\right) + \sum_{j=1,j\neq i}^{N}\sum_{k=1}^{N} \phi_4^{i,j,k} P_k p_j t_i + 1} \tag{14a}$$

$$\text{s.t.} \quad t_i + \alpha_i \leq 1, \quad \forall i \in \mathcal{N} \tag{14b}$$

$$t_i \geq 0, \quad \forall i \in \mathcal{N} \tag{14c}$$

$$0 \leq \frac{p_i}{\eta \alpha_i \sum_{j=1}^{N} P_j |\bar{h}_{j,i}|^2} \leq 1, \quad \forall i \in \mathcal{N}. \tag{14d}$$

$$(11\text{b}),(11\text{c}).$$

where $\mathbf{x} = [\mathbf{P}^T, \mathbf{p}^T, \mathbf{t}^T]^T \in \mathbb{R}_+^{3N}$. The objective function in (14a) can then be expressed as

$$\prod_{i=1}^{N} \frac{u_i(\mathbf{x})}{v_i(\mathbf{x})}. \tag{17}$$

As both $u_i(\mathbf{x})$ and $v_i(\mathbf{x})$ are posynomials, $u_i(\mathbf{x})/v_i(\mathbf{x})$ is not a posynomial, confirming that (14a) is also not a posynomial.

To transform problem (14) into a GP of the form in (12), we would like the objective function (17) to be a posynomial. To this end, we propose to apply the single condensation method [14] and approximate $v_i(\mathbf{x})$ with a monomial $\tilde{v}_i(\mathbf{x})$ as follows. Given the value of $\mathbf{x}^{[m-1]}$ at the $(m-1)$-th iteration, we apply the arithmetic-geometric mean inequality to lower bound $v_i(\mathbf{x})$ by a monomial $\tilde{v}_i(\mathbf{x})$ at the m-th iteration as [14, Lem. 1]

$$v_i(\mathbf{x}) \geq \tilde{v}_i(\mathbf{x})$$

$$\triangleq \prod_{j=1}^{N} \left\{ \left(\frac{v_i(\mathbf{x}^{[m-1]}) P_j p_i t_i}{P_j^{[m-1]} p_i^{[m-1]} t_i^{[m-1]}} \right)^{\frac{\phi_1^{i,j} P_j^{[m-1]} p_i^{[m-1]} t_i^{[m-1]}}{v_i(\mathbf{x}^{[m-1]})}} \right.$$

$$\times \left(\frac{v_i(\mathbf{x}^{[m-1]}) P_j t_i}{P_j^{[m-1]} t_i^{[m-1]}} \right)^{\frac{\phi_2^{i,j} P_j^{[m-1]} t_i^{[m-1]}}{v_i(\mathbf{x}^{[m-1]})}} \tag{18}$$

$$\left. \times \left(\frac{v_i(\mathbf{x}^{[m-1]}) p_j}{p_j^{[m-1]}} \right)^{\frac{\phi_3^{i,j} p_j^{[m-1]}}{v_i(\mathbf{x}^{[m-1]})}} \right\} \times v_i(\mathbf{x}^{[m-1]})^{\frac{1}{v_i(\mathbf{x}^{[m-1]})}}$$

$$\times \prod_{j=1,j\neq i}^{N}\prod_{k=1}^{N} \left(\frac{v_i(\mathbf{x}^{[m-1]}) P_k p_j t_i}{P_k^{[m-1]} p_j^{[m-1]} t_i^{[m-1]}} \right)^{\frac{\phi_4^{i,j,k} P_k^{[m-1]} p_j^{[m-1]} t_i^{[m-1]}}{v_i(\mathbf{x}^{[m-1]})}}.$$

It can be verified that $v_i(\mathbf{x}^{[m-1]}) = \tilde{v}_i(\mathbf{x}^{[m-1]})$. In fact, $\tilde{v}_i(\mathbf{x})$ is the best local monomial approximation to $v_i(\mathbf{x})$ near $\mathbf{x}^{[m-1]}$ in the sense of the first-order Taylor approximation. With (18), the objective function $u_i(\mathbf{x})/v_i(\mathbf{x})$ in (14a) is approximated by $u_i(\mathbf{x})/\tilde{v}_i(\mathbf{x})$. The latter is a posynomial because $\tilde{v}_i(\mathbf{x})$ is a monomial and the ratio of a posynomial to a monomial is a posynomial. The upper bound $\prod_{i=1}^{N} (u_i(\mathbf{x})/\tilde{v}_i(\mathbf{x}))$ of (17) is also a posynomial since the product of posynomials is a posynomial.

Next, we will approximate the constraint (11d) by a posynomial for it to fit into the GP form (12). For this, we lower bound posynomial $\eta \alpha_i \sum_{j=1}^{N} P_j |\bar{h}_{j,i}|^2$ by a monomial as [14, Lem. 1]:

$$\eta \alpha_i \sum_{j=1}^{N} P_j |\bar{h}_{j,i}|^2$$

$$\geq \eta \alpha_i \underbrace{\prod_{j=1}^{N} \left(\frac{P_j \sum_{k=1}^{N} P_k^{[m-1]} |\bar{h}_{k,i}|^2}{P_j^{[m-1]}} \right)^{\frac{P_j^{[m-1]} |\bar{h}_{j,i}|^2}{\sum_{k=1}^{N} P_k^{[m-1]} |\bar{h}_{k,i}|^2}}}_{\triangleq w_i(\alpha_i, \mathbf{P})}. \tag{19}$$

The ratio $p_i/w_i(\alpha_i, \mathbf{P})$ is now a posynomial.

Upon substituting (18) and (19) into (14), we can formulate an approximated subproblem at the m-th iteration for problem (11) as follows

$$\min_{\mathbf{x},\boldsymbol{\alpha}} \quad \prod_{i=1}^{N} \frac{u_i(\mathbf{x})}{\tilde{v}_i(\mathbf{x})} \tag{20a}$$

$$\text{s.t.} \quad 0 \leq \frac{p_i}{w_i(\alpha_i, \mathbf{P})} \leq 1, \quad \forall i \in \mathcal{N} \tag{20b}$$

$$(11\text{b}),(11\text{c}),(14\text{b}),(14\text{c}).$$

In (20a), since $v_i(\mathbf{x}) \geq \tilde{v}_i(\mathbf{x})$ [see (18)], we are actually minimizing the upper bound of the original objective function in (14a). With (19), constraint (20b) is stricter than (11d) as:

$$\frac{p_i}{\eta \alpha_i \sum_{j=1}^{N} P_j |\bar{h}_{j,i}|^2} \leq \frac{p_i}{w_i(\alpha_i, \mathbf{P})} \leq 1. \tag{21}$$

Referring to (12), it is seen that (20) belongs to the class of geometric programming, i.e., a convex optimization problem. Note that the GP (20) is a convex approximation of the original problem (11). In Algorithm 2, we propose a GP-based SCA algorithm in which an instance of (20) is solved at each iteration. The following result gives answer to the second question stated at the beginning of Section III.

Proposition 1: Algorithm 2 generates a sequence of improved feasible solutions that converge to a locally optimal point $(\mathbf{x}^\star, \boldsymbol{\alpha}^\star)$ satisfying the KKT conditions of the original problem (11).

Proof: From (19), we have that $p_i \left(\eta \alpha_i \sum_{j=1}^{N} P_j |\bar{h}_{j,i}|^2 \right)^{-1} \leq p_i/w_i(\alpha_i, \mathbf{P})$. This means that the optimal solution of the approximated problem (20) always belongs to the feasible set of the original problem (11).

Algorithm 2 Proposed GP-based SCA Algorithm

1: Initialize $m := 1$.
2: Choose a feasible point $\left(\mathbf{x}^{[0]} \triangleq \left(\mathbf{P}^{[0]}, \mathbf{p}^{[0]}, \mathbf{t}^{[0]} \right); \boldsymbol{\alpha}^{[0]} \right)$.
3: Compute the value of $v_i(\mathbf{x}^{[0]})$, $\forall i \in \mathcal{N}$ according to (16).
4: **repeat**
5:     Using $v_i(\mathbf{x}^{[m-1]})$, form the approximate monomial $\tilde{v}_i(\mathbf{x})$ according to (18).
6:     Using the interior-point method, solve GP (20) to find an approximated solution $\left(\mathbf{x}^{[m]} \triangleq \left(\mathbf{P}^{[m]}, \mathbf{p}^{[m]}, \mathbf{t}^{[m]} \right); \boldsymbol{\alpha}^{[m]} \right)$ of (11) at the m-th iteration.
7:     Compute the value of $v_i(\mathbf{x}^{[m]})$, $\forall i \in \mathcal{N}$ by (16).
8:     Set $m := m + 1$.
9: **until** Convergence of $(\mathbf{x}, \boldsymbol{\alpha})$

Fig. 3. Topology of the heterogeneous multicell network used in the numerical examples.

Next, since $v_i(\mathbf{x}) \geq \tilde{v}_i(\mathbf{x})$, $\forall \mathbf{x} \in \mathbb{R}_+^{3N}$, it follows that:

$$\prod_{i=1}^{N} \frac{u_i(\mathbf{x}^{[m]})}{v_i(\mathbf{x}^{[m]})} \leq \prod_{i=1}^{N} \frac{u_i(\mathbf{x}^{[m]})}{\tilde{v}_i(\mathbf{x}^{[m]})} = \min_{\mathbf{x}} \prod_{i=1}^{N} \frac{u_i(\mathbf{x})}{\tilde{v}_i(\mathbf{x})} \leq \prod_{i=1}^{N} \frac{u_i(\mathbf{x}^{[m-1]})}{\tilde{v}_i(\mathbf{x}^{[m-1]})}$$
$$= \prod_{i=1}^{N} \frac{u_i(\mathbf{x}^{[m-1]})}{v_i(\mathbf{x}^{[m-1]})}, \quad (22)$$

where the last equality holds because $\tilde{v}_i(\mathbf{x}^{[m-1]}) = v_i(\mathbf{x}^{[m-1]})$. As the actual objective value of (11) is non-increasing after every iteration, Algorithm 2 will eventually converge to a point $(\mathbf{x}^\star, \boldsymbol{\alpha}^\star)$.

Finally, it can be verified that

$$\nabla \left(\frac{u_i(\mathbf{x})}{v_i(\mathbf{x})} \right) \bigg|_{\mathbf{x}=\mathbf{x}^{[m-1]}} = \nabla \left(\frac{u_i(\mathbf{x})}{\tilde{v}_i(\mathbf{x})} \right) \bigg|_{\mathbf{x}=\mathbf{x}^{[m-1]}}, \quad (23)$$

and

$$\nabla \left(\frac{p_i}{\eta \alpha_i \sum_{j=1}^{N} P_j \bar{h}_{j,i}} \right) \bigg|_{\alpha_i=\alpha_i^{[m-1]}; \mathbf{P}=\mathbf{P}^{[m-1]}}$$
$$= \nabla \left(\frac{p_i}{w_i(\alpha_i, \mathbf{P})} \right) \bigg|_{\alpha_i=\alpha_i^{[m-1]}; \mathbf{P}=\mathbf{P}^{[m-1]}}, \quad (24)$$

where ∇ denotes the gradient operator. The results in (23)-(24) imply that the KKT conditions of (11) will be satisfied after the series of approximations involving GP (20) converges to the point $(\mathbf{x}^\star, \boldsymbol{\alpha}^\star)$. This completes the proof. ∎

IV. RESULTS

Fig. 3 shows an example heterogeneous network where all cells have an equal cell radius of 100m. In cells 1 and 3, we set the BS-relay and relay-user distances as 42m and 51m, respectively. In cell 2, the corresponding distances are 42m and 48m. Note that the BS, relay and user in each cell do not lie on a straight line. We set the path loss exponent as $\beta = 3$. For small-scale fading, we assume that the channel coefficients $h_{i,j}$ and $g_{j,k}$, $\forall i, j, k$ are circularly symmetric complex Gaussian random variables with zero mean and unit variance. In the block fading model, the randomly-generated values of $h_{i,j}$ and $g_{j,k}$ remain unchanged in each time block during which the resource allocation takes place. With the channel bandwidth of 20kHz and the noise power densit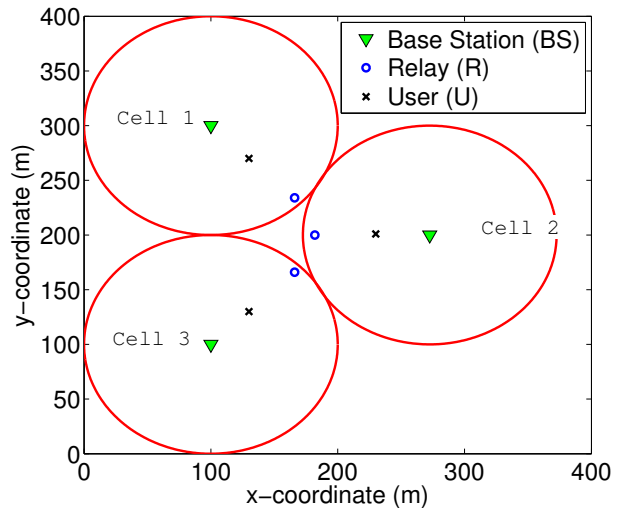y of -174dBm/Hz, the total noise power is $\sigma = -131$dBm. At the relays, we set the energy harvesting efficiency to $\eta = 0.5$ [20]. We initialize Algorithm 2 with $P_i^{[0]} = \varsigma P_{\max}$; $\alpha_i^{[0]} = \varsigma$; $t_i^{[0]} = 1 - \alpha_i^{[0]}$; $p_i^{[0]} = \varsigma \eta \alpha_i^{[0]} \sum_{j=1}^{N} P_j^{[0]} \bar{h}_{j,i}$, $\forall i \in \mathcal{N}$, where $\varsigma \in (0,1)$. To solve each convex problem in Algorithm 2, we resort to CVX, a package for specifying and solving convex programs [21].

Fig. 4 plots the convergence of the network sum throughput $\sum_{i=1}^{N} \tau_i$ by Algorithm 2. Here, each iteration corresponds to solving of a GP (20) by CVX. For all the parameter settings that we consider, it is observed that the proposed algorithm quickly converges in around 4 iterations. As expected, the sum rate is almost doubled when a higher BS transmit power budget of 46dBm is allowed instead of 40dBm. In a multicell network setting, increasing the allowable transmit powers may trigger the 'power racing' phenomenon among the users, thus worsening the interference situation. Our numerical results, on the other hand, confirm that the Algorithm 2 effectively manages the strong intercell interference in such cases and offers a maximized network performance.

It is infeasible to compare the performance of Algorithm 2 with that of a globally optimal solution. There is no global optimization approach available in the literature to solve the highly nonconvex problem (11). A direct exhaustive search would incur a prohibitive computational complexity. However, Fig. 4 shows that the achieved throughput is insensitive to the initial points of Algorithm 2, further suggesting that the attained solution corresponds to the global optimum in our specific example [14], [15].

Fig. 5 demonstrates the advantages of jointly optimizing $(\mathbf{P}, \mathbf{p}, \boldsymbol{\alpha})$ as in Algorithm 2 over individually optimizing the power splitting factor $\boldsymbol{\alpha}$ as proposed in [13]. In the latter approach, we set $P_i = P_{\max}$ and $p_i = \eta \alpha_i \sum_{j=1}^{N} P_j |\bar{h}_{j,i}|^2$, $\forall i \in \mathcal{N}$. To obtain the results presented in the figure, we average the sum throughput over $1,000$ independent simulation runs where we take $\varsigma = 0.5$. For $P_{\max}$ in the range of $43 - 49$dBm, the throughput achieved by Algorithm 2 increases whereas that of [13] does not increase. It is also clear from Fig. 5 that
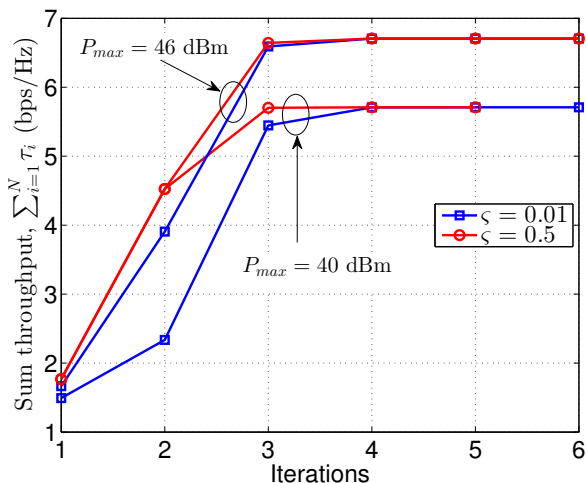
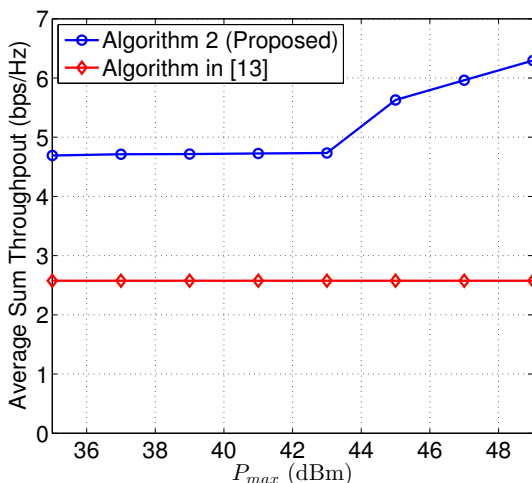Fig. 4.   Convergence process of Algorithm 2.

Fig. 5.   Performance comparison of Algorithm 2 and the proposal in [13].

our proposed algorithm always outperforms that of [13]. Also for $P_{\max} = 46$dBm, which is a typical power constraint value [20], the proposed algorithm achieves double the throughput of algorithm in [13].

V. CONCLUSIONS

This paper has considered the challenging problem of sum throughput maximization in a heterogeneous multicell network with RF-powered relays. Specifically, we have attempted to jointly optimize the BS transmit powers, the relay power splitting factors and the relay transmit powers. To resolve the highly nonconvex problem formulation, we have proposed a successive convex approximation algorithm based on geometric programming. We have proven that the devised algorithm converges

to a locally optimal solution that satisfies the KKT conditions of the original nonconvex problem. Numerical examples have demonstrated the clear advantages of our proposed algorithm over existing approaches.

REFERENCES

[1] J. Andrews, S. Buzzi, W. Choi, S. Hanly, A. Lozano, A. Soong, and J. Zhang, "What will 5G be?" *IEEE J. Sel. Areas Commun.*, vol. 32, no. 6, pp. 1065–1082, Jun. 2014.

[2] Y. A. Sambo, M. Z. Shakir, K. A. Qaraqe, E. Serpedin, and M. A. Imran, "Expanding cellular coverage via cell-edge deployment in heterogeneous networks: Spectral efficiency and backhaul power consumption perspectives," *IEEE Commun. Mag.*, vol. 52, no. 6, pp. 140–149, Jun. 2014.

[3] P. Marsch and G. Fettweis, *Coordinated Multi-Point in Mobile Communications From Theory to Practice*.   Cambridge University Press, 2011.

[4] Z. Chen, B. Wang, B. Xia, and H. Liu, "Wireless information and power transfer in two-way amplify-and-forward relaying channels," *ArXiv Technical Report*, 2013. [Online]. Available: http://arxiv.org/abs/1307.7447v1

[5] Z. Ding, S. M. Perlaza, I. Esnaola, and H. V. Poor, "Power allocation strategies in energy harvesting wireless cooperative networks," *IEEE Trans. Wireless Commun.*, vol. 13, no. 2, pp. 846–860, Feb. 2014.

[6] I. Krikidis, S. Timotheou, and S. Sasaki, "RF energy transfer for cooperative networks: Data relaying or energy harvesting?" *IEEE Commun. Lett.*, vol. 16, no. 11, pp. 1772–1775, Nov. 2012.

[7] Z. Ding, I. Krikidis, B. Sharif, and H. Poor, "Wireless information and power transfer in cooperative networks with spatially random relays," *IEEE Trans. Wireless Commun.*, vol. 13, no. 8, pp. 4440–4453, Aug. 2014.

[8] A. A. Nasir, X. Zhou, S. Durrani, and R. A. Kennedy, "Relaying protocols for wireless energy harvesting and information processing," *IEEE Trans. Wireless Commun.*, vol. 12, no. 7, pp. 3622–3636, Jul. 2013.

[9] H. S. Dhillon, Y. Li, P. Nuggehalli, Z. Pi, and J. G. Andrews, "Fundamentals of heterogeneous cellular networks with energy harvesting," *IEEE Trans. Wireless Commun.*, vol. 13, no. 5, pp. 2782–2797, May 2014.

[10] N. Ksairi, P. Bianchi, and P. Ciblat, "Nearly optimal resource allocation for downlink OFDMA in 2-D cellular networks," *IEEE Trans. Wireless Commun.*, vol. 10, no. 7, pp. 2101–2115, Jul. 2011.

[11] D. W. K. Ng and R. Schober, "Resource allocation for coordinated multipoint networks with wireless information and power transfer," in *Proc. IEEE GLOBECOM*, Austin, TX, USA, Dec. 2014.

[12] K. Huang and E. Larsson, "Simultaneous information and power transfer for broadband wireless systems," *IEEE Trans. Signal Process.*, vol. 61, no. 23, pp. 5972–5986, Dec. 2013.

[13] H. Chen, Y. Li, Y. Jiang, Y. Ma, and B. Vucetic, "Distributed power splitting for swipt in relay interference channels using game theory," *IEEE Trans. Wireless Commun.*, vol. 14, no. 1, pp. 410–420, Jul. 2015. [Online]. Available: http://arxiv.org/abs/1408.3206

[14] M. Chiang, C. W. Tan, D. P. Palomar, D. O'Neill, and D. Julian, "Power control by geometric programming," *IEEE Trans. Wireless Commun.*, vol. 6, no. 7, pp. 2640–2651, Jul. 2007.

[15] J. Papandriopoulos and J. S. Evans, "SCALE: A low-complexity distributed protocol for spectrum balancing in multiuser DSL networks," *IEEE Trans. Inf. Theory*, vol. 55, no. 8, pp. 3711–3724, Aug. 2009.

[16] D. T. Ngo, S. Khakurel, and T. Le-Ngoc, "Joint subchannel assignment and power allocation for OFDMA femtocell networks," *IEEE Trans. Wireless Commun.*, vol. 13, no. 1, pp. 342–355, Jan. 2014.

[17] L. Liu, R. Zhang, and K. C. Chua, "Wireless information and power transfer: a dynamic power splitting approach," *IEEE Trans. Commun.*, vol. 61, no. 9, pp. 3990–4001, Sep. 2013.

[18] A. A. Nasir, D. T. Ngo, X. Zhou, R. A. Kennedy, and S. Durrani, "Joint resource optimization for multicell networks with wireless energy harvesting relays," *ArXiv Technical Report*, 2015. [Online]. Available: http://arxiv.org/abs/1408.4215

[19] S. Boyd and L. Vandenberghe, *Convex Optimization*.   Cambridge University Press, 2004.

[20] X. Lu, P. Wang, D. Niyato, D. I. Kim, and Z. Han, "Wireless networks with RF energy harvesting: A contemporary survey," *IEEE Commun. Surveys Tuts.*, 2014.

[21] M. Grant and S. Boyd, "CVX: Matlab software for disciplined convex programming, version 2.1," http://cvxr.com/cvx, Mar. 2014.